EVALUATION OF THE POTENTIAL IMPACTS OF HYBRID-ELECTRIC AIRCRAFT ON THE GLOBAL AIR TRANSPORTATION NETWORK

Gilbert Tay*, Sarah Gillen*, Raoul Rothfeld, Mirko Hornung*,**
***Technical University of Munich, Germany, ****Bauhaus Luftfahrt e.V., Taufkirchen, Germany**

Keywords: *Technology Evaluation, Hybrid-Electric Aircraft, Air Transport Network Analysis*

Abstract

The potential of hybrid-electric aircraft technology is currently vigorously explored both within the academic community and in industry. The overall technology assessment of a Bavarian research project "PowerLab", which aims to develop a hybrid-electric flying platform, yielded results on its overall application potential. This paper expounds on the application potential of the hybrid-electric aircraft concept of the project "PowerLab" using a network-theoretic approach to analyse the impact on the global air transportation network. The results show the ability of the approach to identify the various network role assignments of the hybrid-electric aircraft application potential. The operational infrastructure requirements for hybrid-electric aircraft operations were analysed in conjunction with the network integration analysis.

1 Topic Motivation and Definition

An important prerequisite in exploring the potential of hybrid-electric aircraft technology is a comprehensive analysis and technology assessment not only at the aircraft level, but also of the operational integration within the air transportation network. The Bavarian research project "PowerLab" aims to create a centre of competence for the development of hybrid and electric aircraft technologies [1]. The project itself aspires to develop core technologies for electrical propulsion systems for turboprops within the weight category of light turboprop aircraft with a MTOW of 4350 kg [1]. The scalability of the developed technologies for larger categories of aircraft was also explored. The application potential for worldwide scheduled commercial air services is explored in this paper in consideration of the full scalability of the developed technologies within the project "PowerLab". The evaluation of such an application potential in the context of this paper is executed in a two-stage process of a macro-level philosophy. Firstly, the representative operational environmental conditions are crystalized and an overall evaluation of the operational environment is performed and infrastructure integration including airside airport capacity is taken into account. For the analysis pertaining to the global relevance of the fleet transport performance, the dataset excludes aircraft types with less than 10 movements per day, thus covering 99.5% of the global available seat kilometres (ASK). Secondly, a macro-level operational fleet network analysis approach is proposed, analysing the representative operational fleets using a network system-of-systems perspective. The network analysis performed uses key parameters characterising the operational network fleets and includes the network topology and network configuration reports. The network analysis complements the operational infrastructure requirements analysis by providing a macro-level view of the network type of operations.

1.1 Hybrid-Electric Application Potential – PowerLab

The hybrid-electric aircraft developed within the PowerLab-Project is an EASA CS-23 type commuter aircraft based on the Dornier Do

128-6 twin-engine STOL utility aircraft. It has a design range of 1850 km (Best-Range-Mission) with a MTOW of 4350 kg. The key technical data of the propulsion and battery systems are shown in Table 1. Due to the current foreseeable implementation of realistic battery energy densities, the battery capacity is sized to enable exclusive battery operation during the take-off run, in the event of a main generator failure [1]. The scalability of the concept is explored to the extent of an ATR-72 type aircraft.

Table 1. Key Technical Data of Propulsion and Battery Systems

Parameter	Data
Service Ceiling	30 000 ft
Max. Power	2 x 300 kW
Max. Continuous Power	2 x 185 kW
Min. Power (OEI)	270 – 290 kW
Min. Power Density (Electrical Motor)	5 kW/kg
Nominal Battery Operation	Take-Off Run for 12s at 260 kW
OEI Battery Operation	Aerodrome circuit of 6 minutes at 260 kW
Storage Capacity	30 kWh
Min. Energy Density	100 Wh/kg
Min. Power Density (Battery)	1 kW/kg
Max. Discharge Depth (DOD)	80%
Lifespan of Battery	>1000 cycles at 80% DOD
Battery Technologies	Lithium-Polymer, Lithium Iron Phosphate

A software tool for comprehensive flight performance and mission analysis of hybrid-electric aircraft was developed to evaluate the transport range and economics of this concept [11]. The analysis considered an initial baseline conservative energy density of 100 Wh/kg and includes computations of energy density variations up to 400 Wh/kg. Results of the mission calculation (see Table 3) revealed a conservative break-even range capability of between 250 km to 500 km and a 16% improvement in overall transport efficiency (kg of fuel per 100 passenger-kilometres) with an increased energy density of 400 Wh/kg, compared to an energy density of 100 Wh/kg as shown in Table 4. These results correspond to the operational range capabilities shown in Figure 5 and Figure 6 and reveal necessary substitution potential considering network range capabilities and transport economics.

Table 2. Overview of reference missions. [11]

Abb.	Payload [kg]	Range [km]
10/50	1000	500
10/25	1000	250
05/50	500	500
05/25	500	250

Table 3. Results of mission calculation. [11]

Abb.	Aircraft Type	Fuel Burn [kg]	El. Energy [MJ]	Total Energy [MJ]	Difference [%]
10/50	Conv. Hybrid	286 288	- 106	13156 13354	1.51
10/25	Conv. Hybrid	161 158	- 104	7406 7372	-0.46
05/50	Conv. Hybrid	279 281	- 101	12834 13027	1.5
05/25	Conv. Hybrid	157 155	- 99	7222 7229	0

Table 4. Key data of the energy density variation with a scaled Hybrid-Do-228-Model [11]

Simulation Hybrid-Do-228				
Energy Density [Wh/kg]	Range [km]	OEW [kg]	Payload [kg]	Transport Efficiency [kg of fuel /(100 Pax-km)
100	250	4335	1444	4.40
	500		1364	4.27
200	250	4176	1588	3.99
	500		1500	3.88
300	250	4123	1636	3.88
	500		1545	3.77
400	250	4096	1660	3.71
	500		1568	3.71

The approach to an overall assessment of the operational environment and elaboration of representative environment conditions are

defined by the parameters used in the context of a "network transport mission" [2], yielding the following operational aircraft clusters [7] as shown in Table 5. The Fleet definition for civilian network transport missions is based on four main parameters - the maximum take-off weight, range, cruising speed and payload. Thus, the global world aircraft fleet was defined based on a database from the years 2008, 2012 and 2014. The solutions were checked for their robustness and validated.

The Do-128 cluster, also referred to here as a "Light Aircraft Cluster", is shown in cluster 7. Other clusters that are eligible for hybridization are highlighted in red. In addition to Cluster 7,

Table 5. Clusters and their description and representatives.

Cluster	Description	Representative
1	Narrowbody	Airbus A320
2	Turboprop	Dash 8Q-400
3	Long Range Widebody	Airbus A330-200
4	High Capacity Freighter	Boeing 747-400F
5	Regional Jet	Embraer 190
6	Mid Range Widebody	Boeing 767-300
7	Light Aircraft	Cessna (Light Aircraft)
8	High Capacity Long Range	Boeing 777-300ER

Cluster 2 ("Turboprop Cluster") is considered as a cluster with hybridization potential.

1.2 Air Transportation Network Design

To understand air transportation networks better, different types of networks are discussed and evaluated. The four most important networks are known as direct network, hub and spoke network, tour network and sub tour network [23].

In direct networks, all spoke cities, are directly connected. A plane starts from city 1 and travels to city 2, from where it returns (without passengers or cargo) to city 1, where it departs again to travel to city 3. The airplane continues this until it has stopped at $5/n$ cities. When it has operated this schedule, the aircraft completes the routing backwards. The advantages of this system are that it ensures that all spoke cities are directly connected. Furthermore, direct service possesses the lowest schedule frequency as well as the highest schedule reliability of all network designs [23].

In a classical point-to-point network, all travellers depart at the flight origin and finish their journey at the destination airport. In contrast to the hub-and-spoke network, all travellers, except for passengers with the hub as their destination, travel to the hub to transfer to a second flight, leading to their destination there. Both systems have advantages that suit certain markets best. This fact makes an eventual predominance of one network system unlikely. [17]

In hub-and-spoke networks, all passengers travel by airplane to a highly connected airport and then catch a flight to their final destinations [23]. These airports are called 'hubs' and have a high number of links to the other airports in the considered network [28]. A plane is dispatched from each spoke city in a certain frequency. When the airplanes land at a hub, they wait for all passengers to change between aircrafts, and subsequently the planes depart to the current spoke city destinations [23]. As a result, hubs must deal with a high volume of traffic at once due to their central connecting role in the network [28]. Consequently, these networks have a high optimal schedule frequency and a low schedule reliability [23]. In free markets (without national or political impediments), airlines generally prefer hub-and-spoke networks to other networks [28]. In general, most airlines operate some combination of point to point and hub to spoke architectures. [12].

In a tour network, each airplane travels from city to city until all have been served. The airplanes travel in a certain direction (clockwise or counter clockwise), leaving for the nearby airport and, after arriving at a city, proceeding to the next airport. The airplane continues this tour along the spoke cities on the circumference until it reaches the last city and retraces its way.

Airlines rarely use this network, but for mass transit and freight trucking it is a common network design. The tour network is an exception of the sub-tour network. [23]

Table 6. Summary of input for network analysis

Network Capacity	Network Cluster 2 (NC2)	Network Cluster 7 (NC7)
Number of flights	471715	208034
Number of flight routes	12480	8088
Number of served airports	2528	1353
Number of edges/links per network	9923	5757
Percentage of overall worldwide network	14 %	3 %

Sub-tour networks consist of one hub airport and n spoke airports, which are split into m subsets (Figure 1). The subsets contain k=n/m neighbouring cities where k must be an even divisor of n. The aim of a sub-tour network is to serve every airport pair and departure/destination airport at the same frequency. In a sub-tour network, passengers travel to a hub by plane, often making several stops at other cities before reaching the hub. At the hub, they take a plane to their destination. [23]

In the network analysis, several different measures are available for use in defining a link. In this case, the following parameters are available: number of flights scheduled, number of flights performed, number of passengers per flight and number of available seats per flight. In the analysis carried out, the number of performed flights per year between airports is selected as the entry for each node pair in the overall transport network adjacency matrix. If at least one such flight is performed annually between airports, a link is created.

Furthermore, the statistical analysis of networks is assigned on networks whose edges have been given a weight and therefore can be described in terms of weighted graphs. Thereby it is possible to provide characteristics of the heterogeneous statistical system and identify the centrality, cohesiveness and affinity of the network. The variable under analysis is represented by the number of direct connections of each airport in the period from November 2007 to the end of October 2008 and will represent therefore the weight w(i→j) of an edge linking airports i and j.

Overall, the network consists of 4 047 nodes (served airports) and 3 828 528 links (recorded flight routes). From this database two clusters of airplanes of the before defined eight will be extracted and analysed. The clusters examined are Cluster 2 (C2) and Cluster 7 (C7). C2 consists of 12 480 flight routes, 471 715 flights and the network serves 2 528 airports while Cluster 7 contains 8 088 flight routes, 20,834 flights serves 1 353 airports per year. This shows that the network of Cluster 2 (NC2) is greater than the network of Cluster 7 (NC7) (Table 6).

In this analysis, the airports under examination will solely be the airports that are served by the airplanes defined in C2 or C7. Consequently, every analysis regarding the network of Cluster 2 will only consider the airports served by Cluster 2. The same applies to C7, where only the airports served by Cluster 7 will be considered for network analysis.

2 Methodology

2.1 Cluster-Based Aircraft and Airport Analysis

The clustering algorithms employed for the aircraft cluster and airport cluster analysis are k-medoid and k-means respectively. The aircraft clustering results are validated and consistent with the results of current publications from our institute. [2] [7]

For the requirements analysis of the airport infrastructure and processes, it is also necessary to determine representative environmental conditions of the airside infrastructure. Figure 1 shows the approach of such an application. After the determination of a representative fleet by means of the aircraft cluster analysis, the aircraft clusters are analysed for their operational impact at the airports. The cluster analysis of the airports helps to better understand the relevant aircraft clusters and to develop further results on their derived operational environments. In addition, it

provides evidential support of a capacity analysis of the airports served, which is necessary for an assessment of the potential for fleet electrification. To perform the analysis, the K-Means algorithm is used using the SPSS analytics software from IBM.

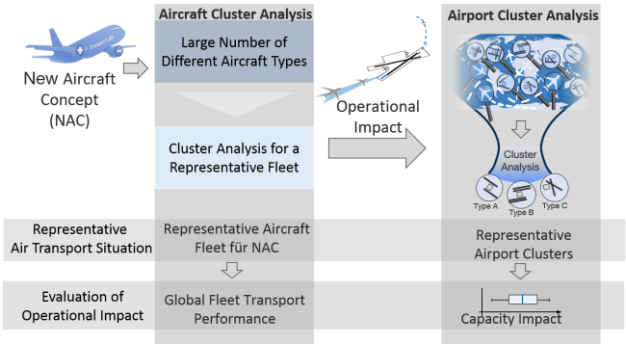

Figure 1. Approach to a cluster-based aircraft and airport analysis. Adapted from [8].

2.2 Operational Fleet-Based Macro-Level Network Analysis

The network analysis is carried out according to the steps defined in Figure 2. First, the parameters for the network analysis are to be defined. For this, parameters are defined to evaluate the previously presented indices according to their usability for the networks under consideration. Secondly, a data definition is carried out, to define the measures for all links and edges. When this is determined, the required data is read out of the database used (OAG database). Third, the airports and routes in the network are defined according to their single node properties. Thereby, the categories "centrality of airports and routes", "relations among airports" and "route patterns" are discussed. Fourth, the global configurations are examined. This is done by a degree distribution analysis. To review the results, a subnetworks configuration examination is carried out.

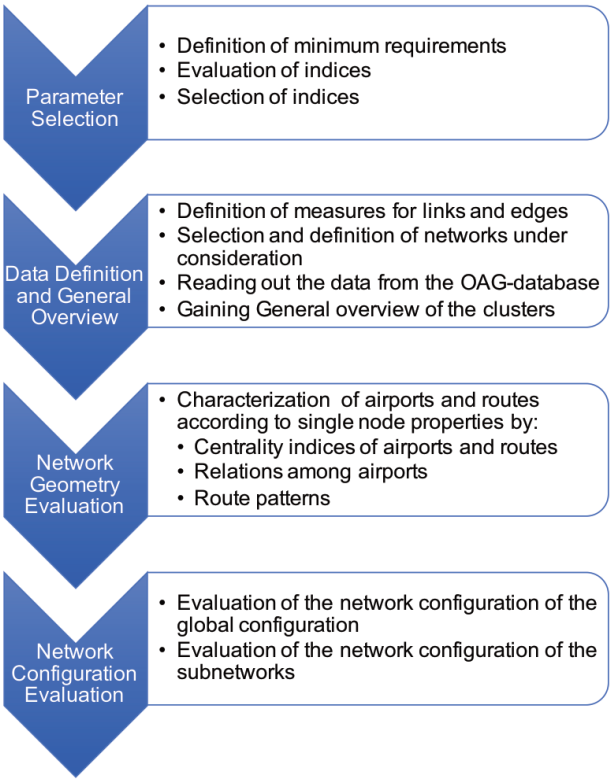

Figure 2. Approach to the network analysis.

The network indices used for the analysis in this paper include the vertex topology indices edge topology and network topology indices. In order to ensure compactness of this paper, the results presented in this paper shall focus on the network analysis as mentioned in section 1.

On the foundation of graph theory stands the network theory. A network is defined as a specific collection of nodes and links with a particular configuration that determines the topology of the network. In a network with N nodes, the topology can be represented by an adjacency matrix A with a size of NxN. Between the nodes of a network, different types of links can occur, including weighted, unweighted, directed and undirected.

For unweighted networks, each link has the same weight, which leads to a binary adjacency matrix. The entries of such a matrix indicate whether a link exists ('1') or not ('0'). [35]

An undirected link means that there is a two-way connection between nodes, which produces a symmetric adjacency matrix. In direct networks, the links represent a one-way connection between the nodes, which produces a non-symmetric adjacency matrix.

In a weighted network, every link is assumed to have an associated scalar weight, which signifies a characteristic property, for example cost, capacity or distance [18]. [35].
The degree k_i of a vertex i in a weighted network is the sum of the weights of the edges attached to it
The local clustering coefficient displays the embeddedness of a single node in a network. A nodes clustering coefficient is defined as the number of triangles centred on a node A_{ij} divided by the number of triples centres on that node k_i. [18]

- **Edge Topology Indices**

Real world networks have a complex network structure and display a heterogeneity in the capacity and intensity of connections in the system. Therefore, it is necessary to assign to each edge of the graph a weight proportional to the intensity or capacity of the connections among the nodes in the network. These data allow to investigate the underlying topology structure of the network as well as information about the correlations in the system. From these results, one aims to determine a better description of the hierarchy and architecture of the weighted network. [15]

The edge betweenness is a measurement of reverse centrality, because it identifies the edges that are most between communities. This information can be used to detect community peripheries in a network [20]. To define the edge betweenness, Ref. 20 generalized the Freeman betweenness centrality for vertices to edges. Thereby it was defined as the number of shortest paths between two nodes that run along an edge. In case of a network that consists of or contains loosely connected communities, these communities are connected by a few intergroup edges. In this case, all shortest paths between the communities must go along one of the connecting edges. These edges show a high edge betweenness that are above average. Underplaying community structures of a network can be revealed by removing edges with high edge betweenness. [20]

- **Network Topology Indices**

The embeddedness e_{ij} of an edge is defined by the sum of the number of nodes that are mutual neighbours of the nodes forming the edge($\sum p_{A\cup B}$). By calculating the embeddedness, it is possible to identify bridges in a network. This is due to the fact that bridges in a network are the edges that own an embeddedness of zero, because the endpoints of the edges have no neighbours in common. [19]
Network topology indices are used to outline geometrical indicators and network shapes of air transportation systems. These indices will be applied on the configurations under investigation, because all complex systems that are characterised by a network structure, share properties entirely depending on the network configuration.
The degree distribution *p(k)* of a network plots the percentage of nodes given in a network with degree k. Through the relative number of nodes by degree given by the degree distribution, a statement about the global structure of air transportation networks can be made. Characteristics of the distribution can indicate how processes on the network may perform, as well as how the network would perform after a node failure. [18]
The diameter D measures the maximum value of the geodesic distances between all nodes in the network. The diameter represents how the links' patterns influence the ability of passengers to move inside an air transportation network. If the diameter is low, the travel distance is reduced, so travellers gain shorter paths to travel between the origin and the destination airport [28].
The global or average clustering coefficient of a network is defined by the mean value of all clustering coefficients in the network [18, 26]. The average clustering coefficient is a measure of the global robustness of a network, which shows a high local connectivity among nodes if it has a high average clustering coefficient and high density [18].
The network density is defined by the ratio of the number of existing links to the number of possible links in the network. High network density in air transportation networks implies higher costs and complexity for carriers. As a

result, it is a design interest to create or find networks with a relatively low density, which are called sparse networks. [18]
The average shortest path length l_{avg}, also called characteristic path length, is the measure of the average separation distance between airports [30]. The formula for the average shortest path length is defined by Ref. 18 and Ref. 16 as follows:

$$l_{avg} = \frac{1}{\frac{1}{2}n(n-1)} \sum_{i \geq j} d_{vt} \tag{7}$$

$$d_{st} = 2 * d_{vt} \tag{8}$$

where d_{vt} is the length of the shortest path between nodes i and j and d_{st} is the geodesic distance between nodes s and t. It is important to have a short average path length in a transportation network [25]. It indicates that any two nodes in a transportation network can be connected in just a few stops. Furthermore, when nodes are well connected and close to each other, clustering occurs [21]. If applied on an air transportation network, passengers prefer a low l_{avg}. The carriers on the other hand, might prefer a longer l_{avg} because if they have a delay, they can compensate for it more easily. [18]

2.3 Network Topology and Graph Clustering

The network topology models of the random network and scale-free models are also implemented as detailed below. Graph clustering methods like modularity clustering [13] and the strongly connected component clustering [14] are applied in order to retrieve comprehensive information from the overall network structure in order to identify subnetworks.

- **Network Topology Models**

An important part of network theory are network models. Models help to understand the behaviour of real world networks, particularly by illustrating the topology through degree distributions. In this chapter, the two main network models, in air transportation systems, are described in more detail. They are called random network and scale free network. [18]

Random networks display homogeneous and sparse patterns with cluster characteristics. Ref. 18 proposed the random network model as the following:

$$P(k) = \binom{n-1}{k} p^k (1-p)^{n-1-k} \tag{9}$$

where κ is the nodal degree and follows a binomial distribution in a random graph with n nodes. If the condition n>>κ is fulfilled, the binomial distribution is approximated by a Poisson distribution, defined by the following equation:

$$p(k) \sim e^{-pN} \frac{(pN)^k}{k!} = e^{-<k>} \frac{<k>^k}{k!} \tag{10}$$

where p represents the connection probability and κ the expected value of the nodal degree, which depends on the connecting probability and network size.

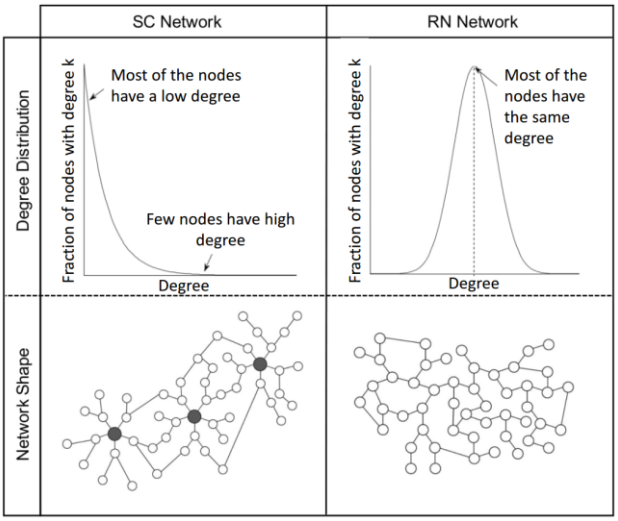

Figure 3. Attributes of a random network (RN) and Scale Free (SF) network. [28]

The nodes in random networks form a homogeneous network topology. The overall number of nodes is assumed to be identical. Therefore, the connection probability remains constant between each pair of nodes [18]. This makes the majority of the nodes accessible in the same way [27]. Therefore, the random network shows a characteristic scale in its degree distribution, characterized by the existence of a peak probability occurring at a particular value of k, which is pictured in Figure 3. The graph shows that the probability of finding highly connected nodes is equal to zero

[18, 27]. This leads to the conclusion that no clear hubs exist and the network configuration seems to be random, since no airport displays a dominant role in the system [27]. In the context of air transportation systems, RNs are used to map point-to-point connections, which are mainly used by low cost airlines [36]. Point-to-Point networks have a low diameter and therefore a high number of links between the airports. They have a high shortest path length and a relatively low average clustering coefficient [28]. The network is more robust to a random node failure than the Scale Free (SF) network, because most of the nodes have a low degree.

The scale free network (SF) introduced by Barabási and Albert was developed to combine principles of growth and preferential attachment upon which many real networks are based on [13]. The Barabási and Albert model (BA-model) focuses particularly on the growth of a network and leads to a scale-free topology [17]. The model takes two properties of a network into account. The first property is the addition of new nodes to the system. The second property is the preferential attachment to generate the power law degree distribution that characterises a scale-free network. This means that new nodes added to the system are much more likely to be connected with nodes possessing a high degree. [18] defined the formula for the scale free BA-Model as follows:

$$P(k) = ak^{-\gamma} \qquad (12)$$

The vertex degree $P(k)$ represents a main feature of the scale free network and follows the power law. It is proportional to $\kappa^{-\gamma}$, where κ stands for the number of links and γ is the degree exponent. γ depends on the attributes of the network and is important to establish the exact network topology, especially the occurrence of hubs. [28] It was suggested that proper hub and spoke networks are only embedded by a SF model if $\gamma = 2$, while for $2 < \gamma \leq 3$, a hierarchy of hubs emerge [14]. For $\gamma > 3$, the hub features are absent and the SF network behaves like a random one. The coefficient *a* depends on the rate of growth and the types of preferential attachments [18]. SF networks include many nodes with few links and few nodes with many links. This forms a heterogeneous network topology and is called a hub and spoke topology, which is less robust to a random node failure. [18] This can be seen in the plot of the degree distribution of a SF network and is pictured in Figure 3. In a SF network the shortest path length is relatively low but the clustering coefficient is high [28].

- **Graph Clustering**

Air transportation networks are often described in terms of complex networks, which consist of a topology of interconnected nodes combining organized and random features. In case of large networks, methods to retrieve comprehensive information from the structure is required. A good way is to decompose the network into sub-units or subnetworks, which are defined as a set of highly interconnected nodes. By identifying these subnetworks, crucial information can be identified and may help to uncover a-priori unknown functional modules. [32] Graph clustering is a method to extract community structures of networks and in the following two different clustering methods are presented.

The modularity clustering introduced by Newman [35] is an algorithm that finds high modularity partitions of large networks in relatively short time. The algorithm is divided into two phases, which are repeated iteratively. The first phase consists of assigning different communities to each node of the network. In the resulting partition, there are as many communities as nodes in the network. Afterwards, the gain of modularity, which is achieved by adding node ***i*** to the community of a neighbouring node ***j***, is evaluated. Node ***i*** will be added to the community for which the gain of modularity is maximum and if no modularity is gained, it stays in the original community. This method is repeated, until no further improvement can be made. The modularity, which is gained by adding a node ***i*** to a community *C*, is defined as:

$$\Delta Q = \left[\frac{\sum_{in} w_i + k_{i,in}}{2m} - \left(\frac{\sum_{tot} w_i + k_i}{2m}\right)^2\right] - \left[\frac{\sum_{in} w_i}{2m} - \left(\frac{\sum_{tot} w_i}{2m}\right)^2 - \left(\frac{k_i}{2m}\right)^2\right]$$

Where $\Sigma_{in}w_i$ is the sum of all weights in community C, $\Sigma_{tot}w_i$ is the sum of all weights of the links which are incident to nodes in C, k_i is the sum of all links incident to node ***i***, $k_{i,in}$ is the sum of weights of the links from node ***i*** to nodes in C and m represents the weight of all nodes in the entire network. If this condition is fulfilled, the first phase is finished and the second phase of the algorithm begins. In this phase, the algorithm builds a new network, which nodes are represented by the communities defined during the first phase. Therefore, the links between two communities are represented by the total weight of all links between the nodes of these two communities. When this is finished, the first phase is applied on the resulting weighted networks.

The strongly connected component clustering (SCCC) can be implemented by the Tarjan algorithm for finding strongly connected components of a directed graph and is introduced by Ref. 29. The algorithm is based on a depth-first search. The search starts from a random node in the graph and visits every node in the network just ones. In the process, the algorithm produces a partition of nodes into the networks strongly connected components, whereby each node appears in just one of the strongly connected components. A node, which is not part of a circle, forms a component by itself. The first node of a component that is identified is called the 'root'.

- **Layout Algorithm**

In this paper, the program Gephi 0.8.2 is used to visualise networks dependencies on their characteristics. Gephi implements various layout algorithms. The layouts are chosen according to the feature that needs to be highlighted in the topology and the size of the network, which sets the shape of the graph.
In the following the layouts are described which are used in this paper.

The Force Atlas Layout is implemented by a force directed graph algorithm, which is based on the simulation of a physical system by defining an attraction force and a repulsion force. According to Ref. 24, force directed algorithms differ significantly by the role played by the distance between two nodes in a graph. Like in physical systems, forces can show a linear, exponential or logarithmic proportionality to the distance between the interacting entities. The Force-Atlas algorithm is based on a linear-linear model (force directed), which means that the attraction force F_a and repulsion force F_r are linear proportional to the distance between nodes in the network. By adjusting the repulsion and the attraction individually, nodes will become either more or less sensitive to other nodes in the network. A high attraction level will force related nodes closer together and a high repulsion will push nodes, which differ a lot, further apart. By adjusting the gravity force, the nodes will be pushed closer to the centre (high gravity) or will be disperse towards the edges (very low gravity). For each network, the parameters vary widely and must be adjusted by iterative processes (1). The Force-Atlas layout can be applied to directed and undirected weighted graphs and is designed to spatialize small world and scale free networks. [22]

Table 7: Layout types implemented in Gephi

Emphasis	Layout
Division	OpenOrd
Complementarities	Force-Atlas 1/2, Fruchterman-Reingold
Rankine	Circular, Radial Axis
Geographic Repartition	GeoLayout

The Fruchterman-Reingold layout is designed for directed unweighted networks. The layout simulates the network as a system of mass particles, where the nodes represent mass particles and the edges are transformed to springs between the particles (nodes). The algorithm is based on trying to minimize the energy of the physical system (network). A disadvantage of the layout is that it operates relatively slow, but it has become a standard in network visualisation. [22]

3 Results of Overall Evaluation

3.1 Representative Operational Environmental Conditions

Figure 4 shows the global ASK, frequency and route shares in 2014 of the different clusters in Table 5. The total coverage of the potential for hybridization of the global transport performance share (ASK share) is approximately 5% if the regional jet cluster is also included. Approximately 32% of the frequency component and 31% of the route component could be covered by possible hybridization if the hybrid Do-128 concept is applied to even larger aircraft. With strict application of the potential hybrid Do-128, the global ASK potential is 0.02% and the global frequency and route potential is 3%.

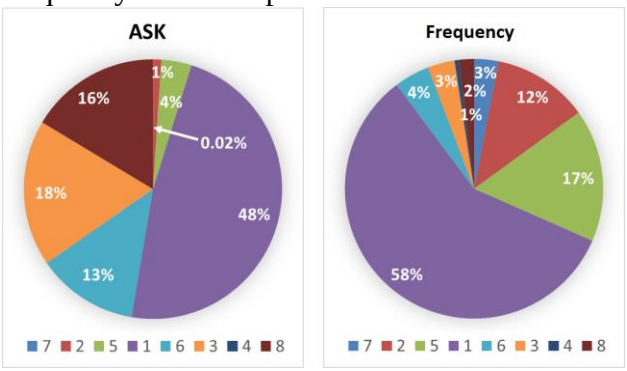

Figure 4. Global ASK and frequency shares according to their respective clusters in 2014.

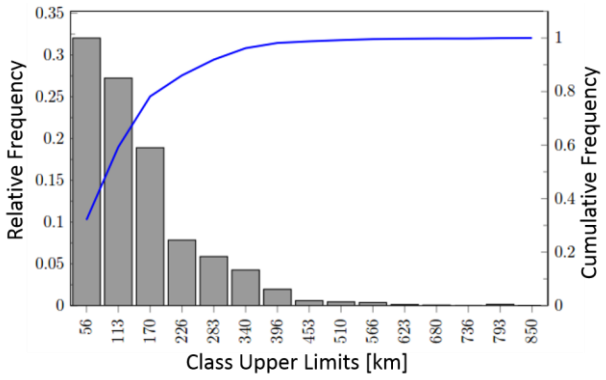

Figure 5. Flown route lengths of Cluster 7 in 2014.

Figure 5 shows that the average flown route length of all flights in 2014 is 160 km and the operational range for a > 90% mission fulfilment is approximately 350 km without reserves. Our study for 2008 also shows that the track lengths have changed only slightly since then. The design range for the hybrid Do-128 of 1850 km (best-range mission) is well above the flown route lengths. For scalability of the concept, the analysis of the flown route lengths of Cluster 2 is shown in Figure 6. Figure 6 shows that the average flown route length of all flights in 2014 is 360 km and the operational range for a > 90% mission fulfilment is approximately 650 km without reserves. Both figures imply that the range capabilities of the concept more than sufficiently meet the operational range requirements. In fact, the design range requirement of the original concept should be further evaluated for future design iterations to better meet demand. The importance of technology evaluation in terms of the elicitation of robust design requirements in early conceptual aircraft design is furthermore underscored.

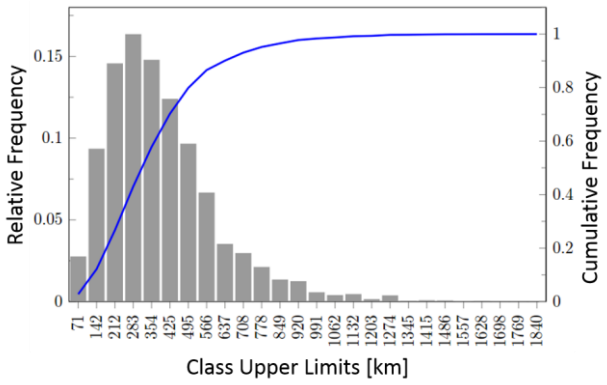

Figure 6. Flown route lengths of cluster 2 in 2014.

3.2 Airport Airside Status Quo Analysis

The objective of this work package is a status quo analysis of the infrastructure and processes and thus an overall comparison and estimation of the operational potential. The impact of the hybrid Do-128 concept on airside operations is an important starting point for the investigation of the requirements analysis of existing infrastructure based on aircraft-specific properties. The airside operation and the runway system of an airport significantly determines the

efficiency of the overall aviation system. This section determines the overall impact of the PowerLab-concept on global airside capacity. A first estimate of the capacity constraint is to be made using a conservative approach. As already explained, this estimate initially refers only to runway capacity. The analysis will provide clues for further analysis in which further aspects of the environmental conditions at the airports can be investigated.

The results of the airport cluster analysis revealed 2 different plausible solutions that are generated by the k-means clustering algorithm implemented in SPSS. These two different solutions are the “2-Cluster-solution” and the “5-Cluster-solution”. In order to critically analyse the results, both solutions are discussed in this section below.

In order to ensure overall clarity, the clustering of the airports performed in this section are called “airport clusters” that differ from the “aircraft clusters” (C1 to C8) in Table 5 and the “network clusters” (NC2 and NC7) in Table 6.

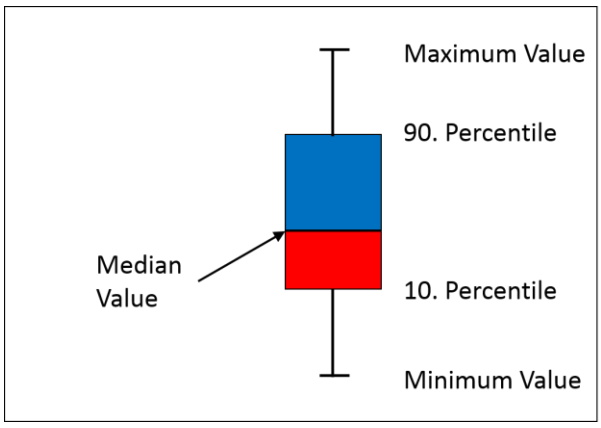

Figure 7. Legend for boxplots in Figure 8 and Figure 10.

Figure 8 shows the 2-Cluster-solution for the airport cluster analysis of the Do-128-Cluster (C7).

The number of airports contained in the first cluster is 678 and in the second cluster is 69. 747 cases are validated and processed. 90.8% of all movements are accounted for by Airport Cluster 1 (left box). From the box plot in Figure 8, it can be seen that over 90% of the airports have less than 20 000 aircraft movements per year. 9.2% of all movements are accounted for by Airport Cluster 2 with the majority of flight movements below 180 000.

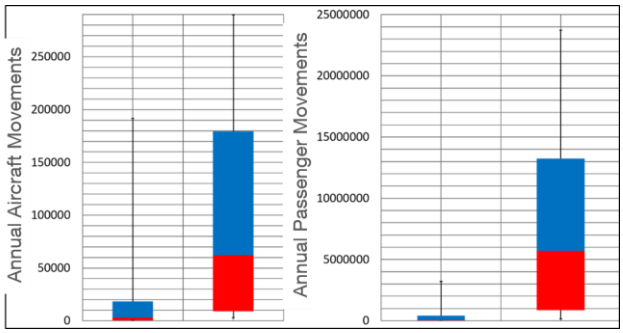

Figure 8. Boxplot of annual aircraft and passenger movements of the 2-Cluster-Solution. Left box is Airport Cluster 1; right box is Airport Cluster 2. See Figure 7 for legend.

Figure 9 shows the aircraft composition in the two airport clusters. From the distribution, it can be seen that the flight operations of the first airport cluster are driven by the "Light Props", i.e. the weight class below the 7 t maximum take-off weight (MTOW). The hybrid Do-128 falls under this weight class. The flight operations of the second airport cluster are dominated by the "medium jets", i.e. the weight class between 7 and 136 t maximum take-off weight (MTOW). The heavy jets belong to the weight class above 136 t maximum take-off weight (MTOW).

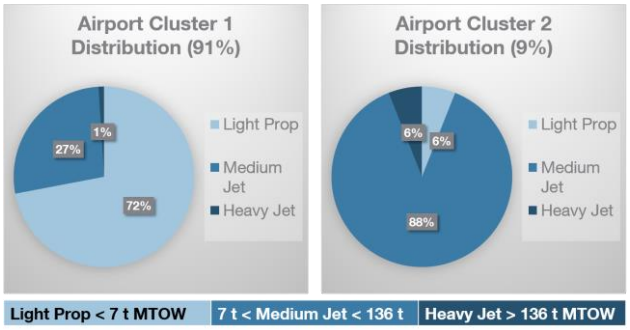

Figure 9. Aircraft distribution in their respective Airport Clusters (2-Cluster-Solution).

Table 16 shows the assessment of airport capacity according to the classification of the FAA [9] with the associated mix index (fleet composition). In Airport Cluster 1, the number of aircraft movements is well below the annual

capacity of a simple single runway system and is not a limitation on flight operations. In this conservative approach, less than 18 aircraft movements per hour in mixed operations (take-offs and landings) are considered as non-critical for the runway capacity [9].

Due to the relatively large spread in the airport cluster 2, the result of the 5-cluster solution is examined more precisely at this point. The result of the 5-cluster solution provides a better insight into those airports that have an above average number of flight movements.

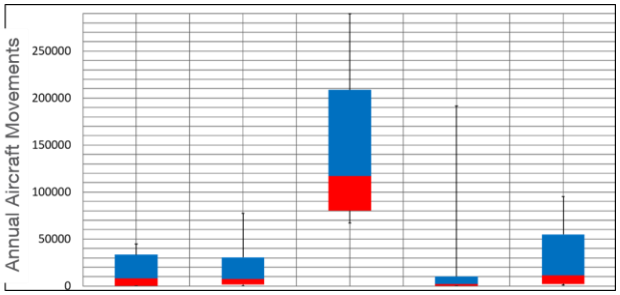

Figure 10. Boxplot of annual aircraft and passenger movements of the 5-Cluster-Solution. See Figure 7 for legend.

Figure 10 and Figure 11 show the results of the 5-Cluster-Solution of the airport cluster analysis. The majority of airport clusters 1, 2, 4, and 5 have fewer than 55,000 aircraft movements in the 90th percentile, and their capacity impact has already been addressed in the second paragraph above. These airport clusters make up approximately 96% of the total airports. For the remaining 4% of the airports in airport cluster 2 (32 cases), most of the movements lie between 80 000 and 250 000 movements.

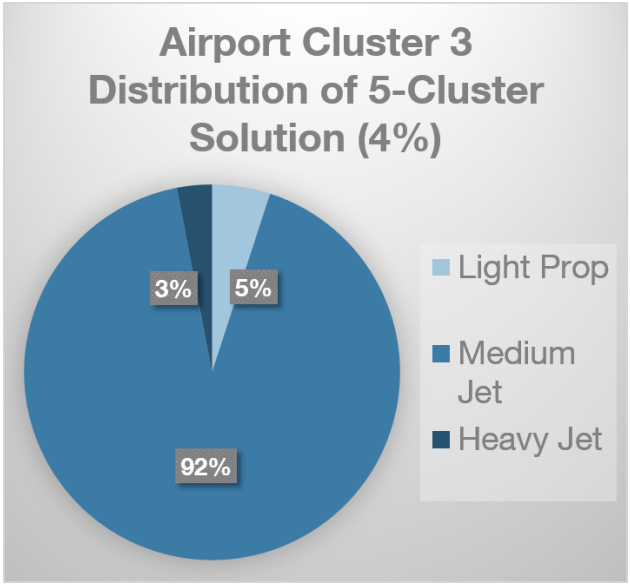

Figure 11. Aircraft distribution of Airport Cluster 3 (5-Cluster-Solution).

An analysis of the aircraft distribution in the airport cluster 2 shows that operations are more than 92% driven by so-called "medium jets", i.e. airplanes with the weight category between 7 and 136 tonnes maximum take-off weight (MTOW). Only 5% of the aircraft in this cluster are in the "Light Prop" category with a maximum take-off weight below 7 tonnes. It can thus be concluded that the airport operational situation is non-critical in terms of airport capacity and does not represent a significant limitation on the operations of the hybrid Do-128.

3.3 Operational Infrastructure Requirements

The battery of the hybridized DO-128 was designed to support the aircraft's take-off procedure. Thus, in the event of a potential failure of the combustion energy generator, the battery should enable electrical continuation of the flight, including a traffic circuit, from the decision point (V1) onwards until the emergency landing. In addition, the battery is designed to absorb power-requirement peaks until cruising altitudes are reached, in order to reduce turbine load. The defined battery usage can, therefore, be divided into three use scenarios: (1) failure of the combustion energy generator during take-off, (2) energy supply for possible performance bottlenecks and (3) energy

Figure 12. Geographical regions according to OAG. [38]

supply during take-off in order to reduce turbine load.

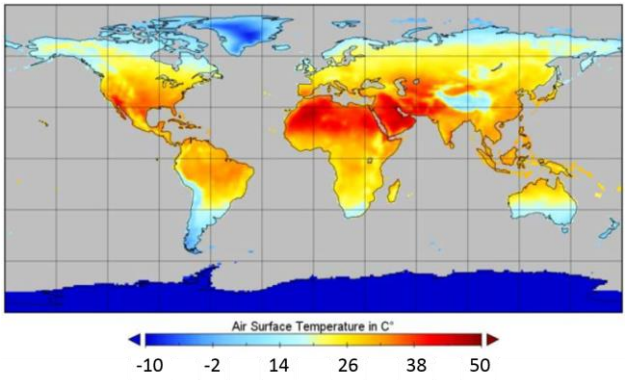

Figure 13. Daily maximum Air Surface Temperatures (15.07.2010) [10]

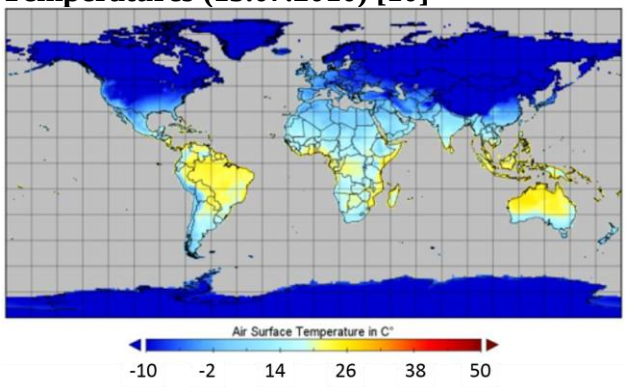

Figure 14. Daily minimum Air Surface Temperatures (15.07.2010) [10]

In the event of combustion energy generator failure during take-off, complete battery draining must be assumed. Due to the failure of one of the main components, a technical inspection of the aircraft is necessary, during which the battery can be charged – without charging being on a critical time path for the aircraft's operation. Due to the high load on the battery during its usage in an emergency case, the maximum battery temperature will be reached if the initial, ambient temperature at before take-off is 20° C or higher. In order to meet system requirements for a hybrid DO-128 to remain operable even with ambient temperature of up to 55° C, active battery cooling is required before take-off, so called (preconditioning). Infrastructure for a hybridised DO-128, therefore, might have to provide facilities for preconditioning of the aircraft's battery. Figure 13 and Figure 14 show the daily maximum and minimum air surface temperatures respectively. Comparing the daily maximum global temperature map in Figure 13 with the geographical locations of the operating clusters in Figure 15 - Figure 18, we see that preconditioning is necessary for most of the routes to be operated on.

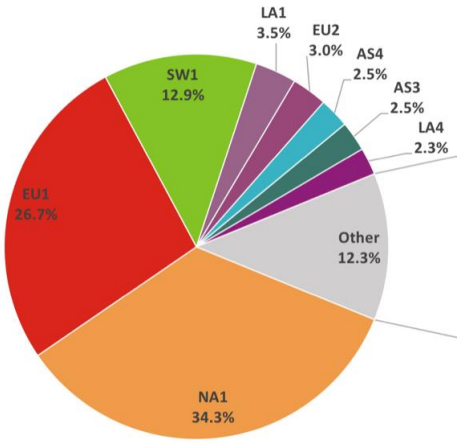

Figure 15. Global route distribution of C2. See Figure 12 for reference.

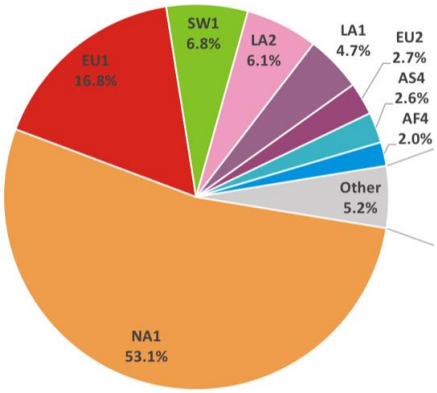

Figure 16. Global route distribution of C7. See Figure 12 for reference.

The use of the battery to provide energy for possible power bottlenecks is only plausible with take-off at maximum range and payload, since the turbine is sufficient as the sole energy source for flight ranges or payloads below the aircraft's maximum. Due to the maximum range of the scenario and the resulting flight length, it can be assumed that the combustion energy generator can charge the battery during cruising flight. Due to the diverting and high load of the battery, preconditioning of the battery remains necessary.

When using the battery to provide energy during take-off to reduce turbine load, the turbine should be operated close to its optimum operating point. In this scenario, it can also be assumed that the battery might be completely discharged during take-off. Therefore, preconditioning of the battery is also necessary in this scenario. As the flight range is not determined by it being a maximum range mission, the possibility of charging the battery during cruising flight might not be fulfilled and results in the need for recharging or replacement processes during the turnaround of the hybridized DO-128. Thus, besides preconditioning facilities, charging or replacement facilities or mechanisms will have to be provided at airports, airstrips, etc. with are intended to allow operation of hybridized DO-128s.

Charging the discharged battery takes up to 50 minutes in an adiabatic environment with maximum allowable charging current and ends with the battery's internal temperature almost reaching the battery's maximum allowable temperature. Time for preconditioning also has to be additionally considered on top of the charging time. However, charging the battery is comparatively less complex than battery exchange and can be carried out in parallel with refuelling. Further, charging requires only limited infrastructure adjustments, as in ensuring availability of ground power or a generator.

Replacing the discharged battery, on the other hand, takes a few minutes, yet can also be carried out in parallel with recharging and allows the battery to be conditioned in advance. However, replacing batteries requires a comparatively complex exchange mechanism (especially for such battery weights of up to 285 kg) and poses additional infrastructure requirements. Battery storage, with cooling and existing battery inventory, and information exchange (e.g. battery stock levels, stored battery types and battery charging levels) at and between all departure airports are required.

Hence considering the time limitations, charging can only be seen as an operationally feasible option if the aircraft utilisation and operational frequency are sufficiently low.

4 Operational Fleet-Based Macro-Level Network Analysis

The results in this section expound on the overall macro-level network analysis of the potential PowerLab hybrid clusters. Figure 17

and Figure 18 provide a geographical overview of global C2- and C7-operations.

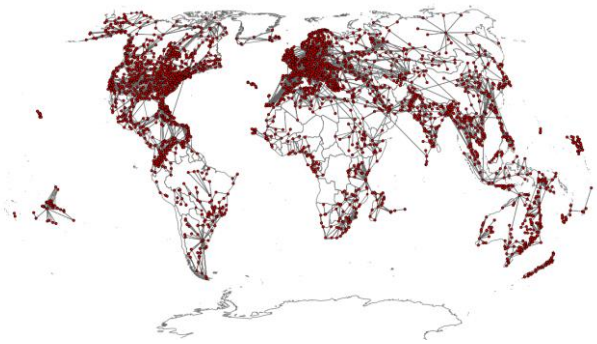

Figure 17. Global overview of C2-Operations.

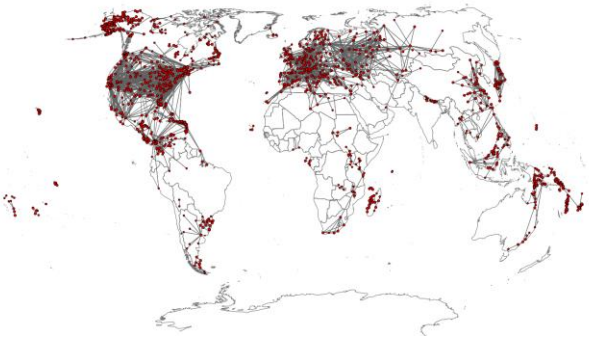

Figure 18. Global overview of C7-Operations.

4.1 Network Configuration and Route Patterns

An important foundation of the network analysis is the accurate knowledge of the actual strength of the edges in a network. In this paper, the weight of an edge is defined as the frequency of flights per year between the initial and the end node. The number of flights is restricted to all flights that were carried out by an airplane defined by rather C2 or C7.

The embeddedness of NC2 shows that the networks exhibits 2850 edges that have the properties of local bridges. This constitutes 29 % of the total number of edges in the network. For NC7 the embeddedness reveals 1562 edges that have the properties of local bridges. This is 27% of the total number of edges of NC2. This shows that both networks have similar fundamental structure regarding the local bridge characteristic. Therefore, both networks are very sensitive to a random edge failure. The neighbouring overlap of an edge considers edges as local bridges, which do not fully meet the requirements. Since both networks exhibit a high number of local bridges, it is unnecessary to examine the neighbouring overlap. The local bridge can be visualised in a Fruchterman layout, which is depicted in Figure 19. Local bridges were highlighted in red and residual edges coloured in blue. By means of this, it can be noted that both networks exhibit the characteristics of direct networks, tour networks and sub-tour. This information is important for the identification of the global composition of both networks.

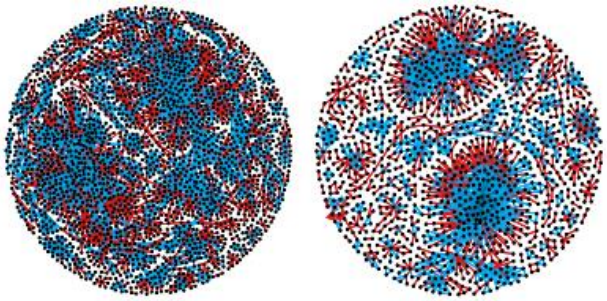

Figure 19. Fruchterman layout of NC2 and NC7 edges sized according to their weight (number of performed flights per year between the initial and the end node). Local bridges are highlighted in red and residual edges are coloured in blue.

4.2 Network Configuration Report

The network configuration report includes the network specific parameters for the determination of network type and the configuration of the subnetwork.

To determine a network configuration, identifying the way nodes in the network are connected is needed. To determine this, one of the key tools called the vertex degree distribution should be used [33]. By the degree distribution function, the most plausible network configuration can be detected. In this section, the networks NC2 and NC7 will be examined according to their tendency to show whether a Gaussian distribution or a power function.

- **Global Configuration Report**

Through the global degree distribution, a statement about the global structure of the networks can be made. For example, how processes on the network may perform, in case of every day operations and in case of an airport

failure. In both networks, hubs clearly exist, but the exact parameters of the distribution cannot be defined. To obtain more precise mathematical statements, the plots of both degree distributions are analysed. Both plots for each network highlight that the data sets better fit a power function. The power function is described by the following formula [28]:

$$f_p(x) = a^*x^b \quad (12)$$

where x represents the degree or weighted degree and the power function coefficient b can be transformed to the power law exponent γ by the following formula [28]:

$$\gamma = 1 + \frac{1}{b} \quad (13)$$

The corresponding R^2, a, b and γ coefficients of the interpolated power functions are listed in Table 8. The R^2 value is a statistic measure of the accuracy of the fitted curve and takes values between zero and one. Values closer to one indicate a better accuracy of the fitted curve.

The networks listed in Table 8 appear to be in a borderline situation, by being between a power fitting and an exponential fitting. The R^2 values for the power function indicate that the data sets fit a power function with relatively high accuracy. The corresponding b coefficient can therefore be used for defining the network attributes of a power-law vertex degree distribution. If the transformation described in equation 12 is carried out, the γ coefficients, introduced in equation 13, can be evaluated. It can be observed that NC2 and NC7 display a power law exponent of 1.987 and 2.297 in their degree distribution, respectively. According to Ref. 5, the value γ = 1.987 indicates that the unweighted NC2 has a proper hub and spoke system, whereas the unweighted NC7 shows, with γ = 2.297, a tendency toward a hub and spoke system but exhibits a hierarchy of hubs.

In contrast, both weighted systems show a higher γ value than the unweighted systems. The weighted NC2 shows a strong hierarchy of hubs in a hub and spoke system and is with the value γ = 3 just in the range of a hub and spoke system. The weighted network of NC7 exhibits a γ value of 3.5 and is therefore located between a hub and spoke system and a random system. It is assumed that NC7 is a hub and spoke system with a very distinct hierarchy of hubs and partly with the characteristics of a random network. If a hierarchy of hubs occurs in a network, it can be assumed that the network has agglomeration patterns.

Table 8: Parameters for power law distribution

	Input Data	R^2	a	b	γ
NC2	Unweighted Degree	0.961	234.3	1.013	1.987
	Weighted Degree	0.994	31.58	0.4963	3.014
NC7	Unweighted Degree	0.956	44.95	0.7709	2.297
	Weighted Degree	0.993	13.42	0.3983	3.510

In conclusion, it can be determined that both unweighted networks show the strongest characteristics of concentration and preferential attachment. Given these partly borderline cases (weighted networks), it is worth to examine these networks more precisely by investigating the subnetwork configurations the networks consist of, which will be discussed in the following section.

- **Subnetwork Configuration Report**

In the previous section, the global network configurations were examined, to enable a statement about the general configuration of the four networks under consideration. To make a more accurate statement about these configurations, the subnetworks, which form NC2 and NC7, will be examined. To do so, the networks will be subdivided by graph clustering. In the following, the Strongly Connected Component Clustering (SCCC) method and the Modularity Clustering (MC) will be implemented.

- **Strongly Connected Clustering Report**

Strongly connected airport communities specified the subdivision of the subnetworks. First, the distributions of the subnetworks will be examined. The graph of C2 was divided into 43 (SN) and the graph of C7 into 80 subnetworks. It can be noted that in both cases the subnetworks are subdivided into two main

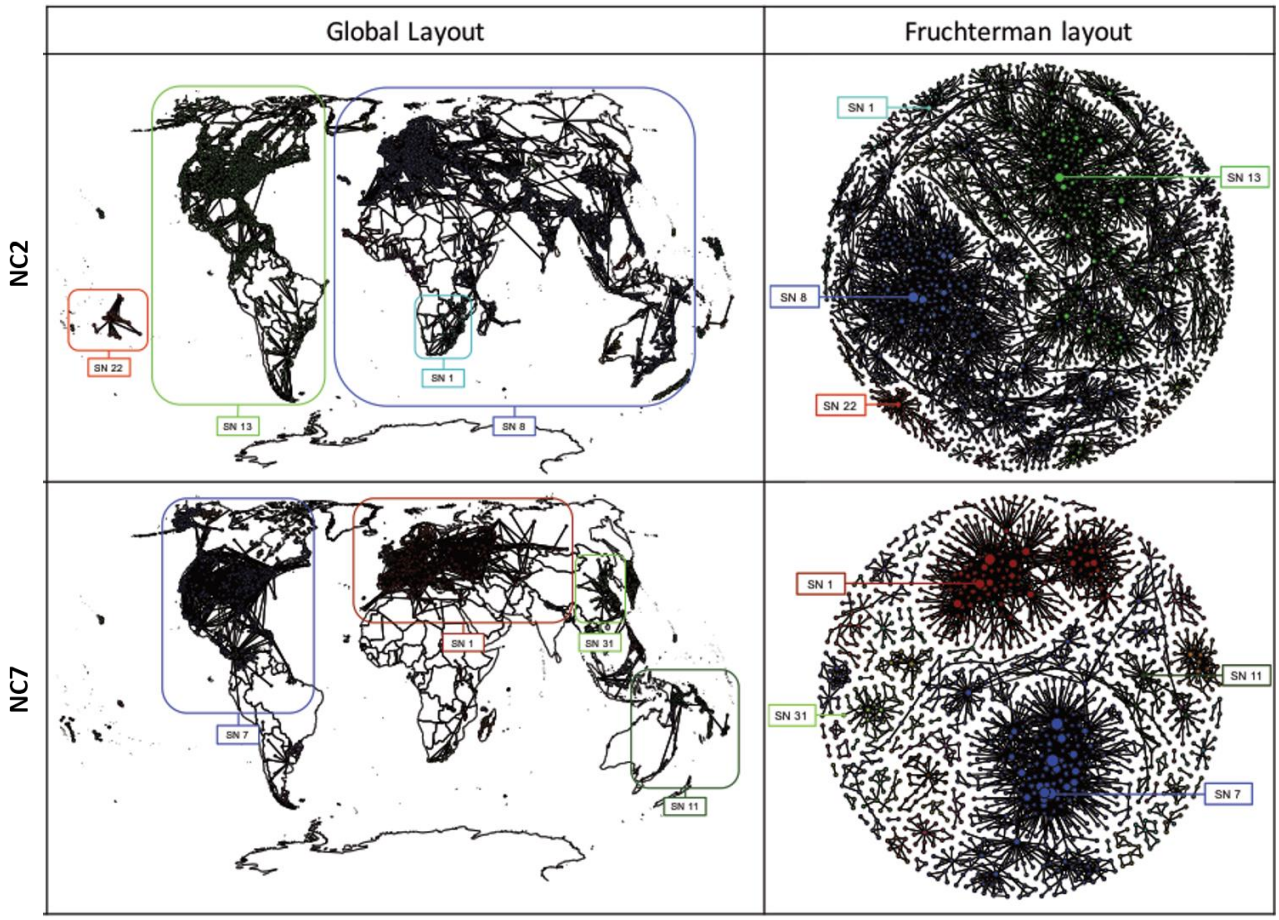

Figure 20. Subnetworks of NC7 and NC7 illustrated on a global map with corresponding Fruchterman layout of NC7 and NC7 with SCCC-subnetworks highlighted by colourisation and hubs highlighted by enlargement.

subnetworks and a large number of relatively small subnetworks. In NC2 the two main subnetworks reach an 85.25% (SN8: 49%, SN13: 36%) share of the total number of nodes. For NC7 the two main subnetworks reach a 54.62% (SN7: 34%, SN1: 21%) share. This means that NC7 exhibits a larger proportion of smaller subnetworks than NC2. This implies an impact on the subnetwork configuration in terms of their connectivity.

By examining the global spatial distribution, information about the structure of the subnetwork distribution can be gained. In Figure 20 the subnetwork distributions are illustrated on a global map.

For air transportation networks, it is important to know if the subnetworks in the system significantly overlap to make a statement about the route behaviour and its implication for the supply, the traffic demand, the airport infrastructure and aviation planning [28]. To examine the mutual interactions between the separate subnetworks, the Fruchterman algorithm was applied on both networks. The results are pictured in Figure 20. It can be observed that the two main subnetworks in NC2 are well connected with small subnetworks but are slightly interconnected with each other. Some standalone networks are also in the subnetworks, which are not connected to any other subnetwork. In contrast to NC2, NC7 consists of many more small networks and the two main networks. The two main networks are not connected with each other and are weakly connected to small subnetworks. The greatest difference between NC2 and NC7 is the interconnection between the small subnetworks in the system. While in NC2 the subnetworks show a relatively average interconnection, in

NC7 the subnetworks mostly stand alone, with just a few exceptions. This can be traced back to the global distributions. In NC2, the two largest subnetworks cover much larger areas and thereby interconnect smaller subnetworks. For NC7, the larger subnetworks are located in different zones and thereby generate a spatial separation.

Now that the composition of the subnetworks is known, the degree distribution can be examined to determine the subnetwork configurations. By investigating the subnetworks, it can be detected if the weighted networks consist of several subnetworks where some show the attributes of random networks and others the attributes of hub and spoke networks. In order to make statements about the configurations, the four largest subnetworks of each cluster were examined. A power fitting was carried out and the resulting coefficients are listed in Table 9. The R^2 coefficients indicate that the transformation, described in equation 13, can be carried out and can be used to evaluate the γ values.

For NC7, the parameters indicate that SN7 is a proper hub and spoke system. SN1 and SN31 are a mixture of a hub and spoke and a random network and SN11 is clearly random. If one considers that NC7 consists of several subnetworks that are not interconnected, as shown graphically in Figure 20, a general assumption for NC7 is not possible. In order to still be able to make a statement about the network, a Fruchterman layout with nodes sized according to the weighted degree has been drawn (Figure 20). It can be noted that, apart from the already considered subnetworks, almost all subnetworks appear to exhibit a random structure with almost zero hubs. 34% of NC7 is a proper hub and spoke network, 24% a mixture of a hub and spoke and random networks and 42% a random network. For NC2, the γ values indicate that SN8 is a hub and spoke network with a hierarchy of hubs, and SN 13 appears to be a random network with partly hub and spoke characteristics. SN 1 and 22 are both hub and spoke networks with random characteristics and a distinct hierarchy of hubs. In order to assess the subnetworks that have not been considered, Figure 20 will be contemplated. It can be noted that these subnetworks appear to have a random and a hub and spoke structure. In summary, it can be retained that NC2 mainly appears to be a hub and spoke network with a hierarchy of hubs but with random network characteristics in the area of SN3 and smaller subnetworks.

○ Modularity Clustering Report

An alternative method of subdividing a network into subnetworks will be applied in the following section and is named the Modularity Clustering (MC). The Modularity clustering specified the subdivision of the subnetworks. The Modularity Clustering introduced by Blondel et al. [32] was used in this paper due to its relatively short operating time and the good accuracy for large graphs. The decision was verified by the modularity of the partition of 0.92 for NC2 and 0.846 for NC7. Both values are close to one and thus indicate a very precise clustering.

The distribution of the modularity clusters shows that NC2 was divided into 58 and NC7

Table 9: Parameters for power law distribution of the four main subnetworks by strongly connected clustering for NC2 and NC7

	Strongly Connected Clustering	Number of Nodes	Percentage share	Average Degree	R^2	b	γ
NC 2	SN08	1235	48.85%	393	0.9934	0.4868	3.054
	SN13	920	36.39%	577	0.9929	0.2044	5.892
	SN01	55	2.18%	269	0.9539	0.4215	3.372
	SN22	34	1.34%	1534	0.9007	0.4365	3.290
NC 7	SN07	453	33.48%	648	0.9965	5.201	1.192
	SN01	286	21.14%	189	0.3847	0.3087	4.239
	SN11	73	5.40%	315	0.8573	0.1442	7.934
	SN31	35	2.59%	109	0.8183	0.2819	4.547

Table 10: Parameters for power law distribution of the six main subnetworks by modularity clustering for NC2 and NC7

	Modularity Cluster	Number of Nodes	Percentage share	Average Degree	R^2	b	γ
NC 2	MC 21	289	11.43%	596	0.9780	0.1020	10.803
	MC 46	159	6.29%	87	0.9377	0.2119	5.719
	MC 49	137	5.41%	177	0.9526	0.1660	7.024
	MC 54	113	4.47%	875	0.5880	0.2136	5.681
	MC 56	109	4.31%	856	0.6309	0.1947	6.136
	MC 57	105	4.15%	439	0.9333	0.2321	5.308
NC 7	MC 85	205	15.15%	822	0.9823	0.2168	5.612
	MC 57	190	14.04%	371	0.9905	0.4586	3.180
	MC 25	97	7.17%	341	0.9580	0.2318	5.314
	MC 50	82	6.06%	146	0.3409	0.1261	8.930
	MC 84	40	2.96%	879	0.5182	0.4321	3.314
	MC 24	35	2.59%	109	0.8183	0.1726	6.793

into 90 subnetworks. As in the strongly connected clustering, NC7 is divided into more subnetworks than NC2. The difference between the two clustering methods lies in the distribution of the number of nodes per subnetwork. While the SCCC method identified two main clusters and a high number of very small subnetworks, the other shows a more evenly divided distribution for the modularity clustering. However, there are still dominating subnetworks, especially in NC7. To examine the subnetworks structure, the six largest clusters with regard to the degree will be examined. These subnetworks reach 36.08% for NC2 and 47.97% for NC7 share of the total number of nodes. The precise percentages per subnetwork can be seen from Table 10.

It can be determined that the subnetworks generated by the MC method are strongly interconnected and partly overlap. Therefore, it is difficult to make a statement about the subnetwork structure based on the global network. To achieve a better overview of the subnetwork structure, the Fruchterman and the Force-Atlas Layout are generated. The Fruchterman Layouts show that in both networks the two biggest subnetworks contain the largest hubs, except for attached smaller subnetworks, which also exhibit smaller hubs.
In order to achieve more information about the structural configuration of the subnetworks it is necessary to consider the Force Atlas Layout, which is pictured in Figure 21 for NC2 and NC7. If the two clustering methods (SCCC and MC) are now compared by means of the Force-Atlas Layouts, it can be noted that for NC7, MC 57 and MC 50 together form SN 1 and MC 85 and MC 25 together form SN7. For NC2 it emerges that MC 21, MC 49 and MC 46 form SN 8 and MC 57, MC 56 and MC 54 together form SN 13. Consequently, the modularity clustering of NC2 rearranges and examines the two largest subnetworks of the SCCC method. In case of NC7, it examines the two largest clusters of the SCCC method more precisely and identifies also smaller unknown parts of NC7. This shows that the MC method subdivides a network into much smaller subnetworks than the SCCC method. Thereby it is possible to make a statement about the behaviour of the network if parts of the networks are removed or fail.

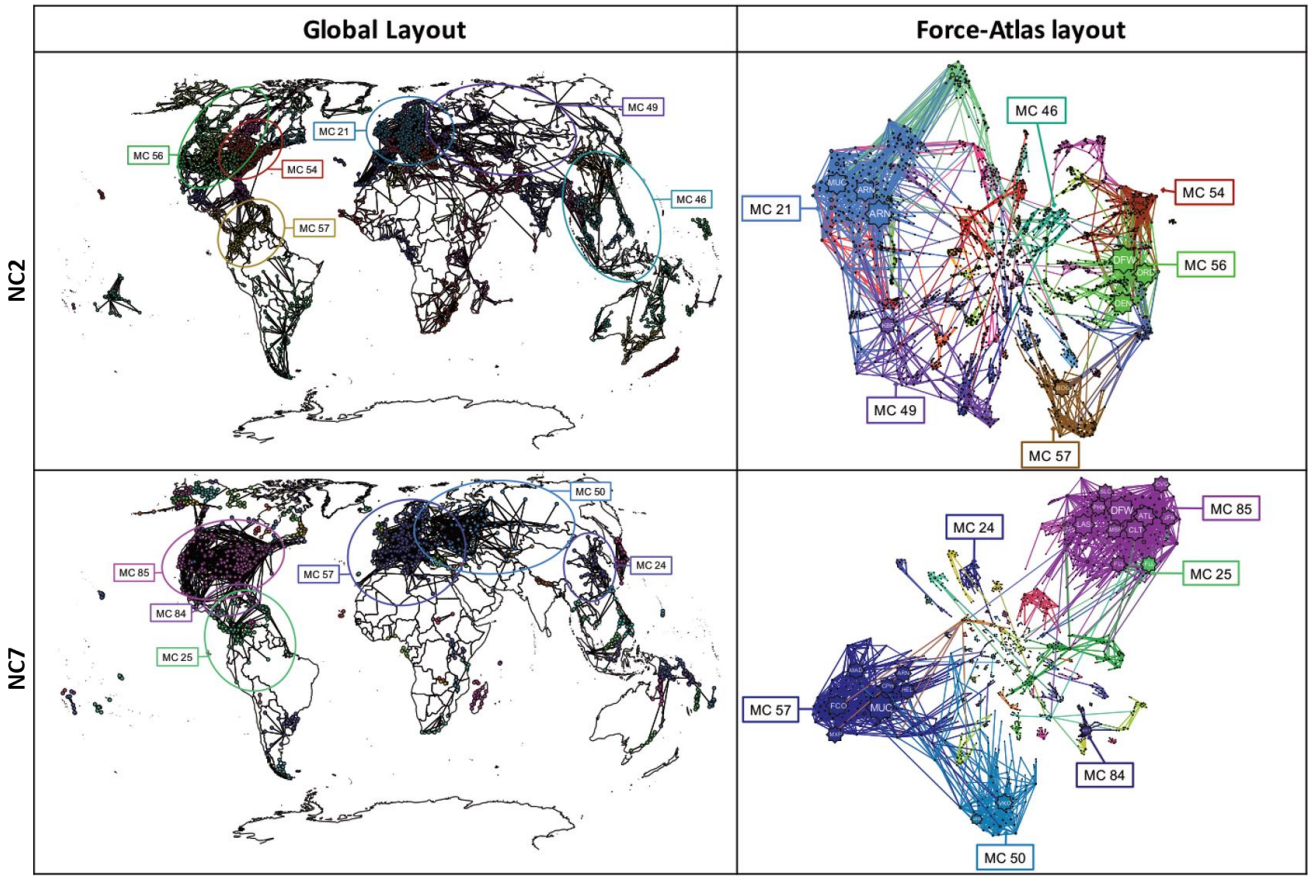

Figure 21. Subnetworks of NC2 and NC7 illustrated on a global map and the Force-Atlas layout of NC2 and NC7 with MC-subnetworks highlighted by colourisation and hubs highlighted by enlargement.

Now, where the composition of the subnetworks is known, the degree distribution can be examined, to determine the subnetwork configurations. The composition of a network can be determined by examining the configuration of the subnetworks. A power fitting was carried out and the resulting coefficients are listed in Table 10. The R^2 coefficients indicate that the transformation, described in equation 13, can be carried out and can be used to evaluate the γ values. The γ values indicates that the six main subnetworks of NC2 range from fully random networks to random networks with partly hub and spoke properties. This may result from the fact that the before examined subnetworks were split up.

For NC2, MC 21 appears to be random, due to the fact that the MC method extracted the strongest airports from SN8 and formed a new cluster. Therefore, the subnetwork emerged from a hierarchy of hubs to a random network. The same applies on the other clusters under investigation, which leads to the fact that if parts of NC2 are removed from the network, it changes from a hub and spoke network to a random one. For NC7, there are also some random characterises on the networks represented for example by MC 50 and MC 24. If parts of the networks are removed, some parts change from a borderline case between a hub and spoke and a random network to a fully random network. In the European area, the greater part of the network stays a hub and spoke network.

Applying the fleet-based network analysis to the airport status-quo analysis (of the operational nodes) in section 3.2, a concurrence pertaining to the network operational characteristics can be implied for the hybrid Do-128-Cluster (C7).

NC7 is characterised by a high number of subnetworks that are mostly stand-alone and two main subnetworks that are not connected to each other and only weakly connected with the

other smaller subnetworks. The operational nodal analysis reveals very low median operational frequency and hence a very low number of rotations. The battery charging variation discussed in section 3.3 concurs with this observation and suggest a higher suitability compared to exchanging the battery, based on macro-level network observations alone.

Regarding the scalability of the concept per se, a similar concurrence cannot be clearly shown. The fleet-based network characteristics of NC2 show a much larger network coverage with a higher interconnectivity and less spatial separation. It is hence an imperative to further determine the exact impact of the charging modality on the aircraft utilisation and rotational frequency in order to clearly define the operational limits for a scalability of the PowerLab concept.

Our approach to a fleet-based macro-level network analysis has demonstrated its use not only in furthering our understanding of air transportation network structures by providing a foundation upon which further research can be conducted but also in evaluating the operational network integration of a hybrid-electric aircraft concept.

5 Conclusion and Outlook

This paper presented a two-stage approach to evaluate the technology potential of a hybrid-electric aircraft concept regarding its impact on the global air transport network. The fleet-based macro-level network analysis provides a foundation upon which the operational characteristics of a fleet-network can be evaluated on a system-wide basis. Evaluating the representative operational environmental conditions revealed the global application potential of the investigated concept. Including the scalability of the concept, up to 17% of the total network could potentially be served. This however excludes the fact that the overall transport performance (ASK) covered is very modest at less than 2%. The airside status quo analysis revealed non-critical operations for such a concept. However, an analysis of the operational infrastructure requirements revealed challenges that need to be overcome for the effective integration and eventual economic feasibility of such a concept.

Furthermore, a macro-level network analysis approach was used to analyse the operational fleet clusters taking into account the network topology and configuration. The network structure of two air transportation systems was investigated by considering several indicators concerning the centrality, topology and connectivity characteristic.

The calculated results point out that both networks can be properly mapped into the Scale-Free Barabási-Model. In particular, NC2 can be formally identified as a mixture of a hub and spoke, a hub and spoke and random network and a random network. NC7 was identified as a dominated hub and spoke network with random network parts. Furthermore, NC2 and NC7 exhibit a hierarchical structure mainly dominated by American and European airports. The moderate hub-and-spoke profile of the European airline network concurs with the mixed structure of this particular network, in which the relatively short distances and transport intermodality play an intermediate role [28]. The executed approach for a macro-level network analysis proved itself a valuable tool for studying the structure of the air transportation system and was able to illustrate emerging complex and interacting network structures.

Both networks under consideration appear to be vulnerable to a random airport or flight route failure. Particularly unfavourable would be the failure of an airport that exhibits a high degree or betweenness. For a flight route, routes, which were defined as local bridges, are especially valuable. Furthermore, a range of airports and flight routes were identified which play significant roles in the air transpiration networks.

The results obtained various characteristic features of the examined networks, but need to be complemented with additional investigations, in particular on the structure and driving forces of the demand side.

References

[1] Jaenker, P., Wollenberg, J., Kastner, N. Development of Electric Drive Trains for Aircraft and Helicopter, Bavarian Research Project "PowerLab", Proceedings of the 10th AIRTEC conference, Munich, 2015.

[2] Tay, G., Kalsi, H., Hornung, M. A Cluster-Based Approach for the Assessment of Air Transportation Networks in Selected Global Regions. 17th AIAA ATIO Conference, Denver, Colorado, AIAA 2017-3773, 2017.

[3] OAG Aviation Solutions, Official Airline Guide Flight Schedules Database 2014, OAG Aviation Worldwide Ltd., 2014

[4] Blondel, V. D., Guillaume J.-L., Lambiotte, R., Lefebvre, E. Fast unfolding of communities in large networks. Journal of Statistical Mechanics: Theory and Experiment. 2008(10):10008

[5] Tarjan, R., Depth-First Search and Linear Graph Algorithms. SIAM Journal on Computing. 1972;1(2):146-60.

[6] Fruchterman, T. M. J., Reingold, E. M. Graph Drawing by Force-directed Placement. Software – Practice and Experience. Vol. 21(11), 1129-1164, 1991.

[7] Tay, G., Michelmann, J., Roß, H., Hornung, M. A Quantitative Scenario-Based Fleet Evolutionary Framework for the Assessment of the Global Air Trnasportation Network. 18th AIAA ATIO Conference, Atlanta, Georgia, 2018

[8] Öttl, G., Impact Evaluation of Air Transport Concepts on Global Airport Operations. TUM Dissertation, ISBN: 978-3-8439-1649-3, Verlag Dr Hut, 2014

[9] Federal Aviation Administration, U.S. Department of Transportation: Airport Capacity and Delay Advisory Circular AC: 150/5060-5, Chapter 1 Par 1-2, 1983

[10] Berkeley Earth. (2016). Data Overview. Retrieved February 26, 2016 from http://berkeleyearth.org/data/

[11] Tay, G., Keller, P., Hornung, M., Development of a software tool for comprehensive flight performance and mission analysis of hybrid-electric aircraft. Vol. 29 (2018), 401-409, Transportation Research Procedia Journal, Elsevier, 2018.

[12] Albert R, Barabási A-L. Statistical mechanics of complex networks. Rev Mod Phys. 2002;74(47).

[13] Barabási A-L, Albert R. Emergence of Scaling in Random Networks. Science. 1999;286(5439):509-12.

[14] Barabasi AL, Oltvai ZN. Network biology: understanding the cell's functional organization. Nat Rev Genet. 2004;5(2):101-13.

[15] Barrat A, Barthélemy M, Pastor-Satorras R, Vespignani A. The architecture of complex weighted networks. Proceedings of the National Academy of Sciences of the United States of America. 2004;101(11):3747-52.

[16] Boccaletti S, Latora V, Moreno Y, Chavez M, Hwang D-U. Complex networks: Structure and dynamics. Physics reports. 2006;424(4):175-308.

[17] Cook GN, Goodwin J. Airline Networks: A Comparison of Hub-and- Spoke and Point-to-Point SystemsAirline. Journal of Aviation/Aerospace Education & Research. 2008;17 Number 2:11.

[18] DeLaurentis D, Han E-P, Kotegawa T. Network-Theoretic Approach for Analysing Connectivity in Air Transportation Networks. JOURNAL OF AIRCRAFT. 2008;45(5).

[19] Easley D, Kleinberg J. Networks, Crowds, and Markets: Reasoning about a Highly Connected World.: Cambridge University Press; 2010.

[20] Girvan M, Newman MEJ. Community structure in social and biological networks. Proceedings of the National Academy of Sciences. 2002;99(12):7821-6.

[21] Guimerà R, Mossa S, Turtschi A, Amaral LAN. The worldwide air transportation network: Anomalous centrality, community structure, and cities' global roles. Proceedings of the National Academy of Sciences of the United States of America. 2005;102(22):7794-9.

[22] Jacomy M, Heymann S, Venturini T, Bastian M. ForceAtlas2, A Graph Layout Algorithm for Handy Network Visualization. 2011.

[23] Lederer PJ. Airline Network Design. Operational Research. 1997;Vol. 46, No. 6(November-December 1998):20.

[24] Noack A. Energy Models for Graph Clustering. Journal of Graph Algorithms and Applications. 2007;11(2):453–80.

[25] O'Kelly M, E. , Miller H, J. The hub network design problem. Journal of Transport Geography 1994;2 (1) 31-40.

[26] Pastor-Satorras R, Vespignani A. Evolution and Structure of the Internet: a Statistical Physics Approach. Cambridge University Press. 2004.

[27] Qiang G, Kun W, Xingli F, Xiaowen F. Why Chinese airlines haven't become leading cargo Carriers - Analyzing air freight network and international trade drivers for mainland China Working Paper ITLS-WP-14-20. 2014.

[28] Reggiani A, Nijkamp P, Cento A. Connectivity and concentration in airline networks : a complexity analysis of Lufthansa's network. Discussion paper / Tinbergen Institute / 3 L, region and environment editor: Rotterdam; 2011. 38 p.

[29] Schaeffer SE. Survey: Graph clustering. Comput Sci Rev. 2007;1(1):27-64.

[30] Tarjan R. Depth-First Search and Linear Graph Algorithms. SIAM Journal on Computing. 1972;1(2):146-60.

[31] Watts DJ. Small worlds: the dynamics of networks between order and randomness. Press PU, editor. Princeton, NJ Duncan J. Watts 2004.

[32] Blondel V.D., Guillaume J-L, Lambiotte R, Lefebvre E. Fast unfolding of communities in large networks. Journal of Statistical Mechanics: Theory and Experiment. 2008(10):10008.

[33] Reggiani, A., Vinciguerra, S., Network Connectivity Models: An Overview and Empirical Applications. In: Friesz T.L. (eds) Network Science, Nonlinear Science and Infrastructure Systems. International Series in Operations Research & Management Science, vol 102. Springer, Boston, MA, 2007.

[34] Erdös, P., Rényi A., On random graphs. I. Publicationes Mathematiques. 1959.

[35] Newman MEJ, Girvan M. Finding and evaluating community structure in netwo rks. Phys Rev E. 2004;69(2)

[36] Cento A. The Airline Industry: Challenges in the 21st Century. 2009

[37] Couto GS, Silva APCD, Ruiz LB, Benevenuto F. Structural Properties of the Brazilian Air Transportation Network. Anais da Academia Brasileira de Ciências. 2015;87:1653-74.

[38] OAG Aviation Solutions, Official Airline Guide Flight Schedules Database June 2008, UBM Aviation Worldwide Ltd.,

Acknowledgements

The authors would like to acknowledge the support provided by the Free State of Bavaria for this research. (Funding number: LABAY75E)

Contact Author Email Address

Gilbert.tay@tum.de

Copyright Statement